How to Use Metallurgical Analysis for Fire Investigation: The Case of AISI 316 Stainless Steel

Andrea Casaroli, Marco Boniardi, Riccardo Gerosa and Barbara Rivolta ⓘ*, Dipartimento di Meccanica, Politecnico di Milano, Via G. La Masa, 1, 20156 Milano, Italy

Abstract. In this work, fire simulations were carried out on AISI 316 austenitic stainless steel sheets (similar to EN X5CrNiMo17-12-2), usually employed for the production of flue pipes. The thermal alteration induced by the fire was simulated by heating samples at different temperatures (from 20°C to 1050°C) and for different exposure times (1 h and 6 h) in a laboratory furnace. The metallurgical investigation concerned the surface coloring by photographic analysis; the morphology and chemical composition of the surface oxides by SEM and EDS; the microstructure as a function of temperature by LOM. The influence of the different parameters was discussed by a statistical ANOVA approach. The obtained results allowed to associate each temperature to one or more alterations in color, to the morphology and the chemical composition assumed by the surface oxides, as well as to the microstructure of the steel.

1. Introduction

The main method to investigate and determine the causes of a fire is the visual analysis. The generated heat, in fact, damages the objects and leaves traces related to the modification of their mechanical properties and the surface aspect.

During the investigation, the consultants focus the attention on for main aspects: (I) the fire ignition causes, (II) the starting point, (III) the fire development modality and (IV) the temperature reached by the fire [1–3]. The investigation of these points often requires a lot of information related to the consequences of the flames in the area involved in the fire (fire patterns) and the witnesses present in the accident place. The main consequences of the fire on the surrounding structures can be divided in two types: the movement patterns that are related to the fire path and the intensity patterns, related to the intensity of the flames [4].

Some examples of the movement patterns are the distance made by the flames on horizontal surfaces (floors or wood bases), the deformations of the light bulbs

---

*Correspondence should be addressed to: ; Barbara Rivolta, E-mail: barbara.rivolta@polimi.it

(pulled light bulbs) [5], the reduction of the mechanical properties of the mattress springs or the traces left by the heat reflected by objects that stop the fire movement (heat shadowing) [6]. Moreover, other information can be obtained by the marks left by the hot gases on the ceiling. Such traces can be represented by a surface blackening or, in case of very high heat sources, by zones in which the concrete start to split apart (spalling) [7].

The most common examples of intensity patterns are instead the degree of carbonization of the wood surfaces [8], the calcination degree of the plasterboard walls and the fires plumes patterns [9] produced by the hot gases, by the flames and by the fumes. Generally, such evidences are truncated cone shaped and represent the boundaries of the flames, the hot gases and the fumes with the building walls.

By means of the observed evidences, it is possible to recreate the fire path by a vectorial diagram.

The most frequent method employed to determine the temperature reached during the fire is the presence of melted or partially melted plastic or metallic objects. The first ones are characterized by melting temperatures included among 90°C and 350°C. Usually, they can give useful information only if they were located in zones touched slightly by the fire. The metallic objects, instead, are characterized by higher melting temperatures, about 420°C to 490°C for zinc-aluminum alloys (domestic control valves, stove burners, etc.), 650°C, 550°C to 650°C for aluminum alloys (window frames, ventilation ducts, etc.) and 1400°C to 1500°C for steels (bed springs, beams, fasteners, bolts and nuts, etc.). If melting is the only one reference to estimate the fire temperatures, only the aluminum or zinc-aluminum alloy components can be considered, since the temperatures during a fire rarely exceed 900°C to 1000°C.

Nevertheless, metallic materials give a further important advantage: the surface oxide and the microstructure are characterized by features and transformations well associated with the temperature; they can be studied and observed carefully by optical and electronic microscopes [10–12]. These can represent valid instruments for scientific investigations that are increasingly required beside the visual analysis.

However, it is often complicated to find accurate data and technical information for a comparison with the obtained results.

As said before, the metallurgical features of the metallic alloys can be used to estimate the temperatures reached during a fire, since they are stable and don't change during the extinguishing [13–15].

The present paper aims to remark the potentiality of the metallurgical analysis during a fire investigation [16–19]. Fire simulations were carried out on AISI 316 (similar to EN X5CrNiMo17-12-2) stainless steel sheets usually employed for flue pipes. Fire developed from chimneys are in fact frequent. Moreover, stainless steels flue pipes are always present in houses or industrial buildings and are characterized by constant properties among the product available on the market.

2. Materials and Methods

AISI 316 sheets were subjected to a simulated fire heating them in a laboratory furnace. It should be noted that the furnace used for the experimental tests is not able to recreate the low oxygen atmosphere typical of confined fires. However, this limitation can be considered trifling for the present investigation because, in most cases, the fires affecting the flues are not confined and develop from the roof ensuring the presence of an oxidizing atmosphere for the whole duration of the fire.

The treatment required three stages:

– Quick increase of the temperature up to the desired level;
– Soaking for two different times, 1 h and 6 h;
– Air cooling.

After the heating stage, each specimen was subjected to the following analysis:

– Visual and photographic examination of the sheet surface color;
– Microscopic analysis of the oxide morphology and chemical composition by scanning electron microscope (SEM) and EDS probe;
– Metallographic investigation by light optical microscope.

The visual examination was carried out by two digital reflex cameras inside a suitable white chamber. The obtained pictures were initially analyzed using the X-Rite Colorchecker Passport Photo® system [20], in order to make the color independent of the used camera, and then by a Matlab® algorithm specifically developed to determine the red–green–blue (RGB) color channels histograms. The data were employed to build a digital image in the RGB color space. The average color data were then studied by the ANOVA analysis aiming to investigate the influence of the temperature, of the heat exposure time and of the camera on the specimens' color tonality. This procedure minimized the influence of the environment on the color of the acquired images.

The SEM analysis was employed to study the oxide morphology and the chemical composition (by EDS probe). Finally, the microstructure modifications occurred during the tests were investigated by metallographic analysis.

The data obtained from the present experimental plan will be useful to understand carefully the temperature interval reached by a chimney or a sheet component exposed to a fire.

2.1. Photographic and SEM Analyses

In order to study the true color of a sheet after a fire objectively, a wide experimental survey was determined by a random factorial plan with two repetitions per each tested condition. Three parameters were considered: the fire temperature, the heat exposure time and the camera employed for the image acquisition.

The investigation was carried out with 13 temperature values included among 20°C and 1050°C; this temperature is reached during a fire rarely, but it was con-
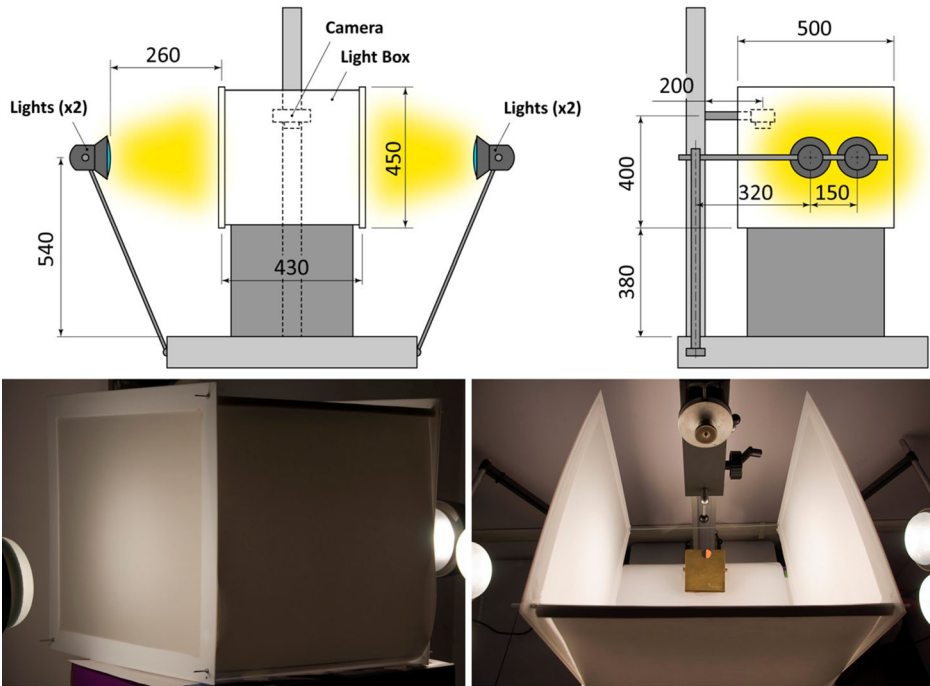
Figure 1. Sketch of the photographic system.

sidered as maximum limit. The selected temperatures (20°C, 150°C, 225°C, 300°C, 340°C, 375°C, 415°C, 450°C, 525°C, 600°C, 750°C, 900°C, 1050°C) were related to significant variations of the surface color. The heat exposure time was fixed at 1 h and 6 h: the first one was chosen to compare the results with the British Stainless Steel Association data [21], whereas the second one was selected to study the surface condition in case of long lasting fires. The images were captured by two different reflex cameras: a Canon EOS 450D and a Nikon D300. The final experimental plan is hence made by 52 specimens and 104 pictures.

The specimens are 80 mm side squares cut from an AISI 316 sheet 0.6 mm thick with a 2B surface finishing [22]. Before each test, the specimens were cleaned carefully. They were put inside the laboratory furnace when the selected temperature was reached. The cooling occurred in free air. Because of the thin thickness, the heating and cooling times were very limited.

All the pictures were taken on a suitable photographic system (shown in Fig. 1) including four 150 W incandescence lamps and a light box able to diffuse the light uniformly. The cameras were fixed at 400 mm from the observed sheet eliminating all the others light sources [23].

The comparison of the pictures taken by the two cameras was performed after a suitable calibration able to reduce the influence of the camera. The images, saved in the RAW format, were analyzed using a X-Rite Colorchecker Passport Photo® calibration system made by 24 colors (Fig. 2) and by a specific software.

Figure 2. Image of the X-Rite Colorchecker Passport Photo®. Each one of the 24 targets is characterized by a pure, flat and intense color.

In order to create a reference image for the picture calibration, a photograph of the X-Rite target was taken in the same light conditions adopted for the experimental specimens.

This reference image was used by the X-Rite Colorchecker Passport Photo® software for the calibration of the pictures, in the raw format, captured by the two cameras. The pictures coming from the X-Rite Colorchecker Passport Photo® software were finally saved in the PNG format, using an 8-bit depth for each color channel. In this way, each color channel is represented by 256 values: 0 represents the black color and 255 the pure color. The RGB histograms and the related average values were calculated by a specific algorithm developed with the software Matlab® (Fig. 3). Before the metallographic analysis the specimens were also observed by a Zeiss EVO 25 scanning electron microscope to study the oxide morphology and chemical composition.

The ColorChecker Passport Photo® allowed to reproduce the color faithfully under any light source and with different types of cameras. It consists of a support on which 24 color samples are printed using high quality inks, formulated to reproduce the real color of natural objects in all components of the visible spectrum.

This aspect is fundamental if the purpose is to objectively link the color assumed by the AISI 316 stainless steel sheets to the temperature to which they were exposed during the fire. Otherwise, the color tone could be distorted by the type of light of the environment, its intensity and the type of camera used for taking the photos.

The calibration involved three phases:

1. A photo was taken at the ColorChecker Passport Photo® under the same lighting conditions as in the lightbox for all plates.
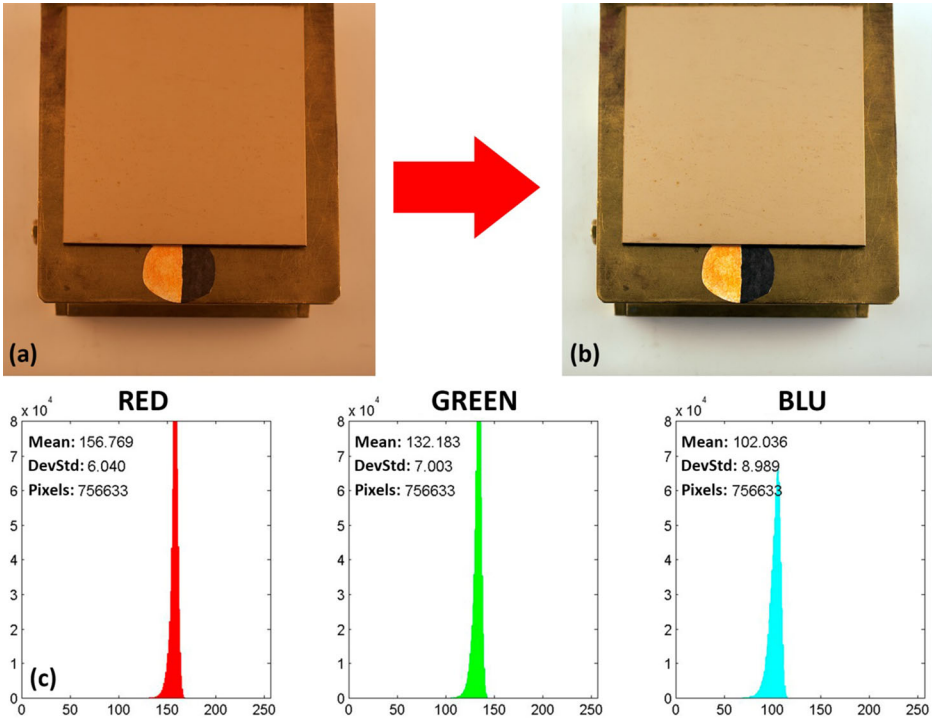
Figure 3. Original image (a) and after the color calibration by Colorchecker Passport Photo® system. (b–c) RGB histograms calculated by the Matlab® algorithm. The x-axis shows the colour hue of an 8-bit image while the y-axis highlights the number of pixels that have a specific colour hue.

2. The specific color profile was created for the two cameras used during the experiment. The profiles were generated using ColorChecker Camera Calibration software and resulted in the method required for image calibration.
3. The color profile was applied via Lightroom® software to all RAW files of photographs taken under the same lighting conditions and with the same camera.

For maximizing the efficacy of the calibration process, particular attention was paid to using the same lighting mode through the light box. All the photos in the ColorChecker Passport Photo® were taken from the front while maintaining the position and distance between the target and the camera. The framing was also selected so that the ColorChecker Passport Photo® would occupy about 60% of the image.

The light box and the calibration process allowed to eliminate the effect of the environment and the camera on the color of the sheets but did not allow to

remove the influence of the calibration of the screens or printers used for the images view.

As the calibration of each device was not practically feasible, the color of the sheets was characterized through the histograms of the three channels (red, green and blue) defining each color in the RGB space.

This procedure allowed to create a unique reference, useful for each investigator to estimate the temperature reached by the AISI 316 stainless steel sheet. Both the images and the RGB histograms shown in Figs. 4 and 5 represent a quick and objective reference with which to compare the images taken of the finds collected at the site of an accident. The only care required is to take photos of the finds through a common light box and using an appropriate color calibration system.

The ANOVA analysis of the histograms shown in Figs. 4 and 5 allowed to establish which experimental conditions actually produced a color tone that was statistically different from the others.

The histograms were obtained by an appropriate algorithm developed in the Matlab® environment. The algorithm analyzes the hue of each color channel (red, green and blue) of each single pixel that constitutes the photograph to which it assigns a value between 0 (black) and 255 (pure color).

At the end of the analysis, the algorithm builds the histogram by counting the number of pixels that have assumed a specific value for each color tone. The x axis represents the value of the color tone (from 0 to 255 for 8bit images), while the y axis highlights the number of pixels that have a specific tone.

2.2. Metallographic Analysis

Specimens parallel and perpendicular to the rolling direction were taken from each sheet. The cutting was carried out very carefully to prevent microstructural modifications. After the standard polishing operation with abrasive papers and 3 μm and 1 μm diamond cloths, the samples were etched by a solution containing HCl (45 ml), HNO_3 (15 ml), glycerol (3 ml) and water (30 ml). The microstructure was finally observed by a LEICA® DM4000M optical microscope.

3. Results and Discussion

3.1. Photographic Analysis

Figures 4 and 5 show some of the specimens subjected to the described tests. The heating time of 1 h is reported in Fig. 4, whereas the 6 h soaking specimens are visible in Fig. 5. Each image is associated to the related RGB histograms, the average values and the standard deviations.

The averages and the standard deviations of the color channels were subjected to the ANOVA analysis in order to determine which of the following parameters, temperature, heat exposure time and used camera, is significantly able to influence the sheets color. It was assumed that two colors are statistically different when also their RGB channels averages are different.

Figure 4. Specimens heated for 1 h at 20°C, 375°C, 450°C, 600°C, 900°C, 1050°C. All the pictures are calibrated with the Colorchecker Passport Photo® system. The x-axis shows the colour hue of an 8-bit image while the y-axis highlights the number of pixels that have a specific colour hue.
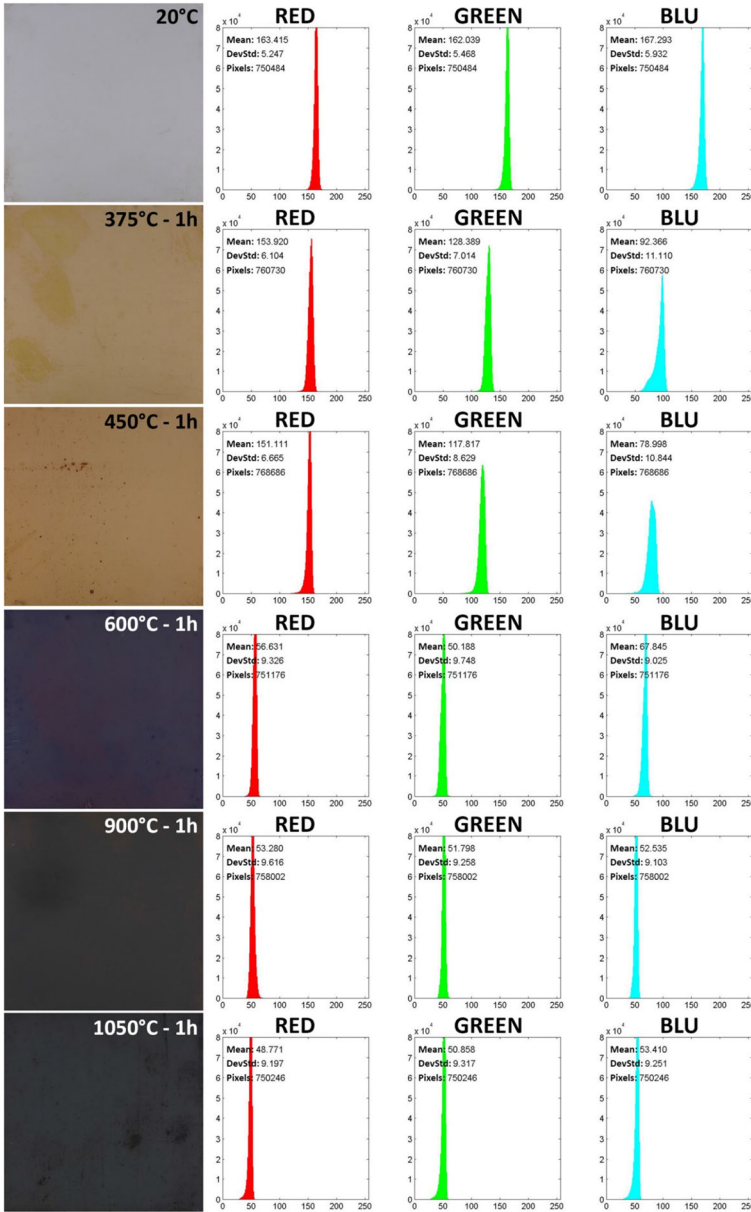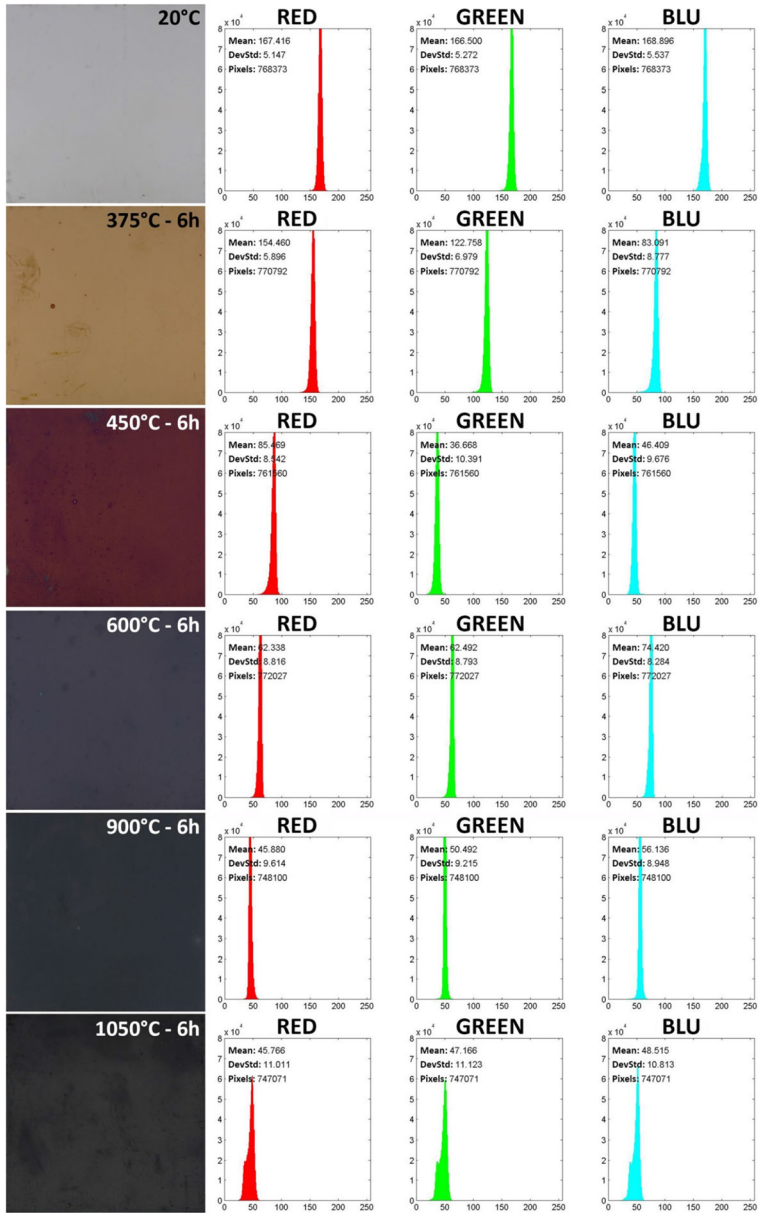
Figure 5. Specimens heated for 6 h at 20°C, 375°C, 450°C, 600°C, 900°C, 1050°C. All the pictures are calibrated with the Colorchecker Passport Photo® system. The x-axis shows the colour hue of an 8-bit image while the y-axis highlights the number of pixels that have a specific colour hue.

The average of a color channel can be calculated as average of all the intensities of the image pixels related to that specific color. The standard deviation is instead related to the dispersion of the data around the average value. The preliminary data processing shows that the influence of the employed camera is negligible and the one of the heat exposure time is very limited. The temperature, instead, proved to be the most important parameter. The analysis pointed out that there are two temperature intervals, 20°C to 340°C and 900°C to 1050°C, in which the colors are not significantly different, whereas among 375°C and 750°C the data change rapidly probably because of some stains with very different color in respect to the rest of the specimen.

Aiming to investigate a possible interaction among the considered parameters, a deeper ANOVA analysis was carried out. Three main factors, three double interactions and one triple interaction were considered. Moreover, a Bonferroni approach was employed to obtain a test with a total significance (α) equal to 5%. This procedure requires a significance level α_{fam} per each test, that is equal to α/I, where l is the number of comparisons ($\alpha_{fam} = \alpha/I = 0.05/7 = 0.00714$) [24].

The results confirmed the influence of the temperature, of the heat exposure time (strong for temperature and more limited for the time) and of the combination of these two parameters, whereas the choice of the camera proved to be negligible.

After the previous analysis, the Tukey test was employed to compare the experimental exposure time–temperature conditions. Tukey test determines the individual means which are significantly different from a set of means. It is considered as a multiple comparison test and is applicable when there are more than two means being compared. Tukey test is used after ANOVA to show that significant difference exists and determine where the difference exists. Tukey test is calculated through a pairwise comparison of all means. The aim was the determination of the ones characterized by significantly different RGB channels.

The performed analysis was finally used to determine the exposure time–temperature combinations that result in a not discernible color. In order to understand the previous result better, in Fig. 6 the data referred to 1 h and 6 h exposure time were separated into two different plots. For the test time of 1 h, the colors cannot be distinguished in the temperature intervals of 20°C to 340°C, 375°C to 415°C and 900°C to 1050°C. For the 6 h data, instead, the temperature intervals are 20°C to 225°C, 340°C to 375°C and 900°C to 1050°C.

3.2. SEM Analysis

The SEM analysis was performed on the stainless steel sheets before preparing the samples for metallographic analysis. The SEM analysis carried out on the sample at 20°C, showed the presence of a surface layer of oxide containing Fe–Cr-Ni and Mo, naturally formed from AISI 316 stainless steel. The oxide layer is thin, compact and well adherent to the surface. The samples submitted to 1 h soaking time (Figs. 7 and 8) don't show any significant variations neither of the morphology nor of the oxide chemical composition till 600°C.
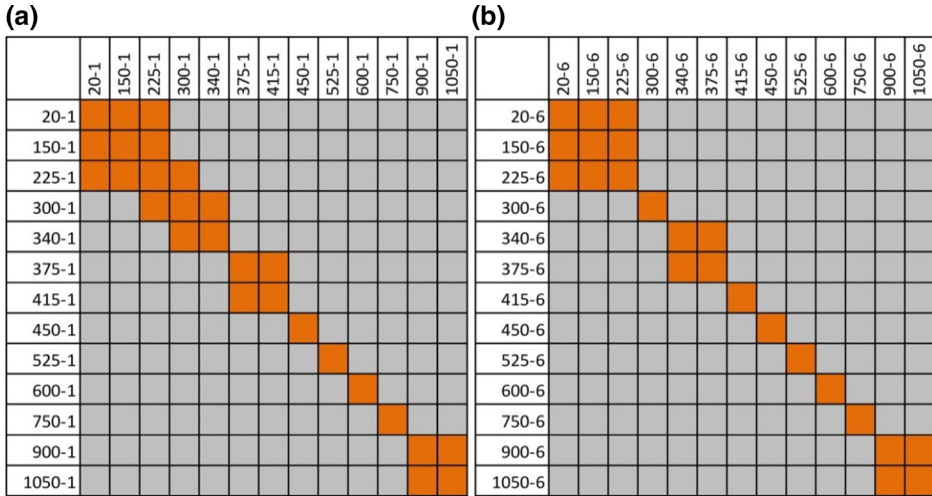
(a)

	20-1	150-1	225-1	300-1	340-1	375-1	415-1	450-1	525-1	600-1	750-1	900-1	1050-1
20-1	■	■	■										
150-1	■	■	■										
225-1	■	■	■										
300-1				■	■								
340-1				■	■								
375-1						■	■						
415-1						■	■						
450-1								■					
525-1									■				
600-1										■			
750-1											■		
900-1												■	■
1050-1												■	■

(b)

	20-6	150-6	225-6	300-6	340-6	375-6	415-6	450-6	525-6	600-6	750-6	900-6	1050-6
20-6	■	■	■										
150-6	■	■	■										
225-6	■	■	■										
300-6				■									
340-6					■	■							
375-6					■	■							
415-6							■						
450-6								■					
525-6									■				
600-6										■			
750-6											■		
900-6												■	■
1050-6												■	■

Figure 6. Experimental exposure time–temperature conditions with the same statistical color (orange boxes) for 1 h (a) and 6 h (b) test durations.

The effects of the high temperature oxidation become evident starting from 750°C. From this temperature the oxide layer starts to grow a lot and shows an enrichment of Chromium and Oxygen at the expense of Iron, Nickel and Molybdenum. Also the shape of oxides changes significantly: till 600°C the oxide is smooth and compact, starting from 750°C it becomes rough and it tends to flake off easily. The increase of the oxide thickness continues both at 900°C and at 1050°C, further enriching with oxygen and chromium and gradually occupying the whole surface of the sample.

The samples submitted to 6 h soaking time (Figs. 9 and 10) show a similar behavior, even if the abnormal growth of the oxide already starts at lower temperature (600°C).

3.3. *Metallographic Analysis*

Before the metallographic investigation, chemical analysis were performed by optical emission spectrometer on 4 samples not submitted to heating. The results (Table 1) show that the chemical composition agrees with the prescriptions of ASTM A240 Standard for AISI 316 steel grade.

The metallographic analysis of the samples at 20°C shows an equiaxial austenitic grain fully recrystallized of 20 µm average size. The metallographic analysis does not show any difference between the transversal and longitudinal direction. In Figs. 11 and 12 only the specimens taken from the longitudinal direction are reported. Up to 525°C the microstructure remains unchanged, regardless of the exposure time.

Between 600°C and 750°C, on the other hand, a strong precipitation of chromium carbides occurs at the grain boundary. This phenomenon is typical of AISI 316 stainless steel and occurs when the steel is subjected for prolonged times to
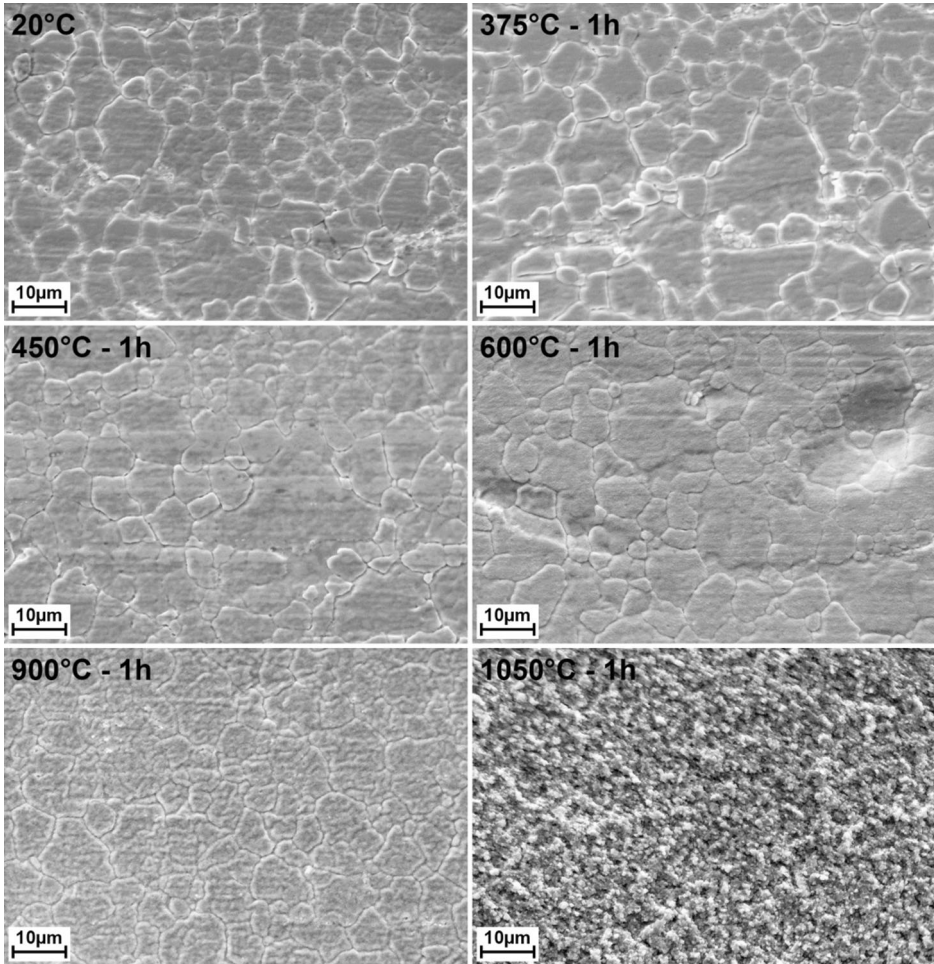
Figure 7. Surface oxide morphology of the sheets heated for 1 h at 20°C, 375°C, 450°C, 600°C, 900°C, 1050°C. SEM analysis (4000×).
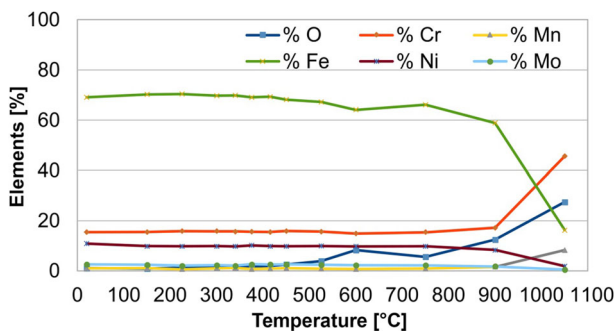

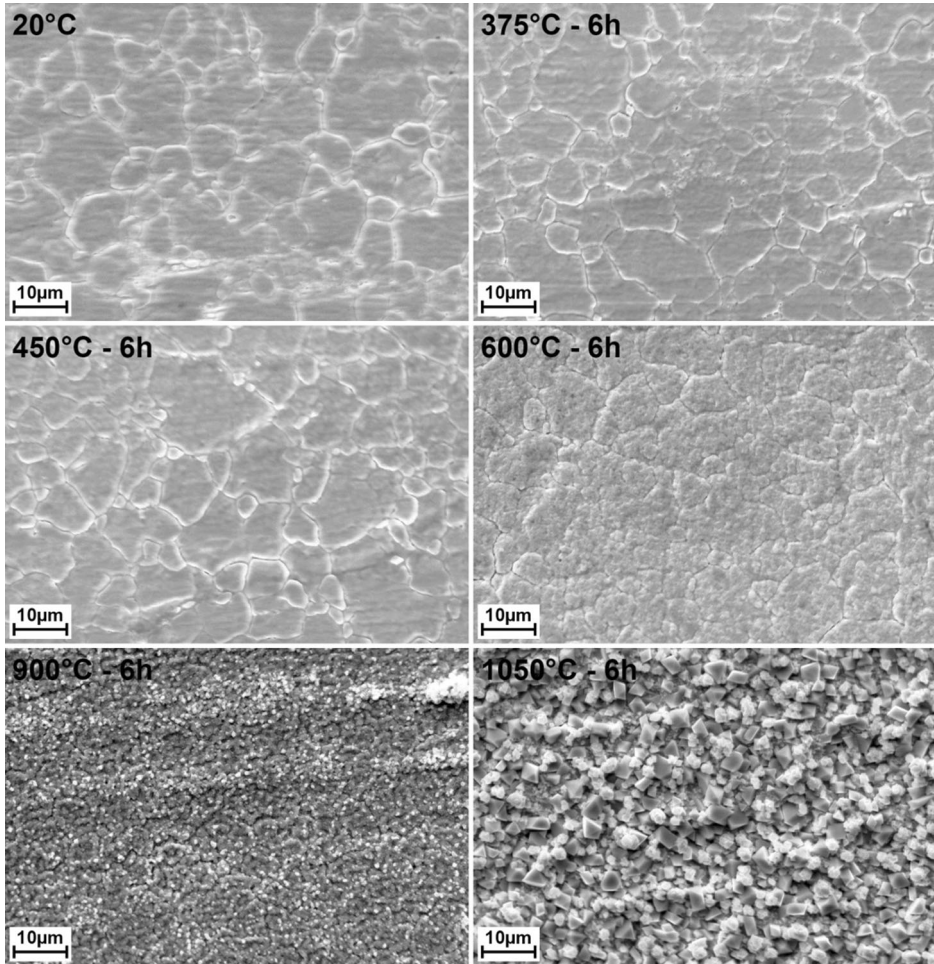**Figure 8. EDS chemical analysis of the 1 h soaking surface oxide.**

Figure 9. Surface oxide morphology of the sheets heated for 6 h at 20°C, 525°C, 600°C, 750°C, 900°C, 1050°C. SEM analysis (4000×).

temperatures between 500°C and 800°C, with a maximum at around 700°C. The precipitation of carbides therefore represents a clear experimental evidence, through which to identify the temperature range reached by the stainless steel in the event of a fire.

At 900° C the temperature is too high to allow the precipitation of chromium carbides on the grain boundary which are totally absent. The grains appear strongly enlarged and, in some areas, they are larger than 60 μm. At 1050° C, the grain further increases, assuming an average size bigger than 100 μm. Only limited differences were observed between the tests conducted with an exposure time of 1 h and those at six hours.
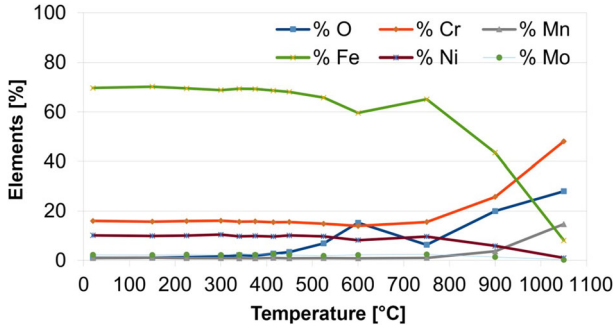
Figure 10. EDS chemical analysis of the 6 h soaking surface oxide.

Table 1
Chemical Analysis Performed by Optical Emission Spectrometer on Four Samples Not Subjected to Heating

	C [%]	Mn [%]	P [%]	S [%]	Si [%]	Cr [%]	Ni [%]	Mo [%]	N [%]
Sample 1	0.06	1.37	0.03	0.005	0.36	16.89	10.10	2.11	0.01
Sample 2	0.06	1.40	0.03	0.004	0.35	16.92	10.09	2.15	0.01
Sample 3	0.06	1.37	0.03	0.004	0.36	16.82	10.09	2.13	0.01
Sample 4	0.06	1.39	0.03	0.006	0.35	16.84	10.11	2.17	0.01
Standard	0.08	2.00	0.045	0.030	0.75	16.0	10.0	2.00	0.10
	Max	Max	Max	Max	Max	18.0	14.0	3.00	Max

The results show the compliance of the sheets with the ASTM A240 standard for AISI 316

4. Conclusions

In this work, fire simulations were carried out on AISI 316 austenitic stainless steel sheets (similar to EN X5CrNiMo17-12-2) usually employed for the production of flue pipes. Fires generated from chimneys are in fact very frequent. Stainless steel flue pipes are also always present in homes or industrial complexes and are characterized by constant properties among the products available on the market.

The samples, 80 mm × 80 mm side, were obtained from a cold rolled sheet with a thickness of 0.6 mm and a 2B surface finishing. On each sample, the thermal alteration induced by a fire was simulated by heating at different temperatures (from 20°C to 1050°C) and for different exposure times (1 h and 6 h).

The surveys conducted through ANOVA statistical analysis concerned:

– The surface coloring;
– The morphology and chemical composition of the surface oxides;
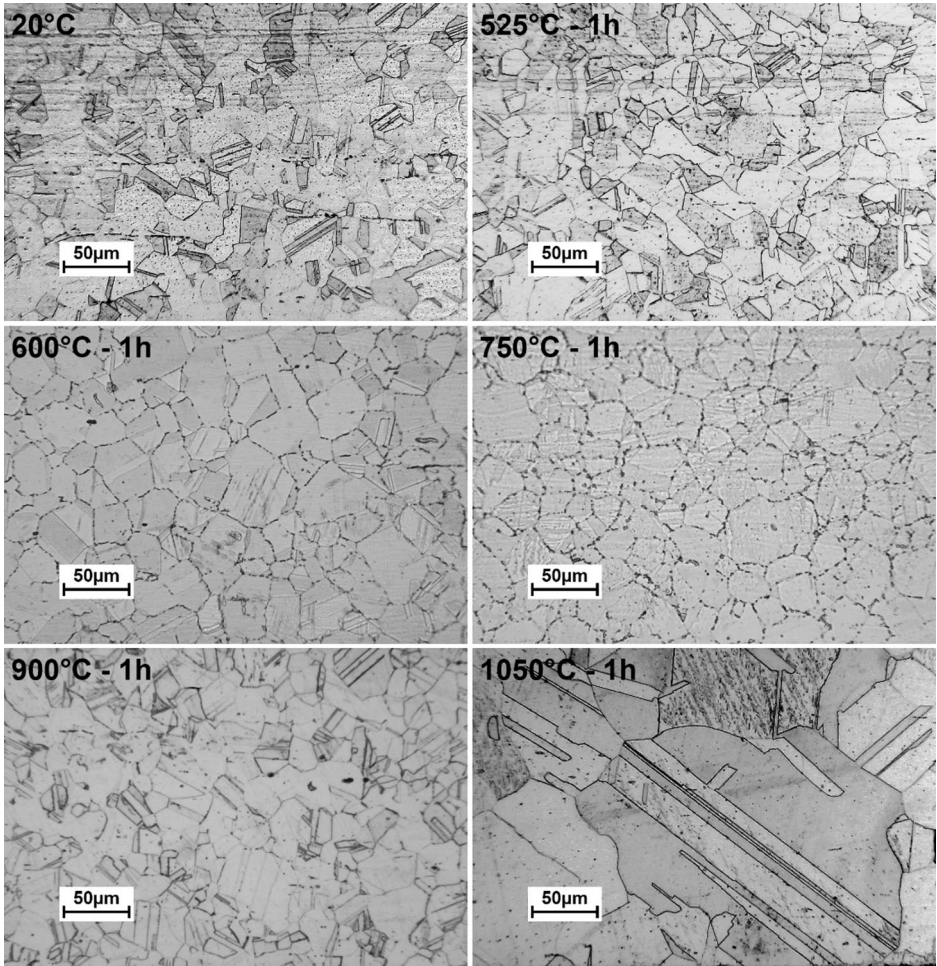– The microstructure as a function of temperature.

Figure 11. Metallographic survey on the longitudinal direction of the specimens heated for 1 h at 20°C, 525°C, 600°C, 750°C, 900°C, 1050°C (200×). The etching was carried out by a solution containing HCl—45 ml, HNO₃—15 ml, glycerol—3 ml and water—30 ml.

This type of analysis made it possible to associate each temperature to one or more alterations in color, to the morphology and the chemical composition assumed by the surface oxides, as well as to the microstructure of the steel.

With regard to the statistical analysis of the color, the possibility of making the images tone independent from the environment in which the photograph is taken, was demonstrated. It has also been demonstrated that the color assumed by the sheet depends on the temperature, the exposure time and their interaction. The samples heated to six hours in fact have thicker surface oxides and a darker color than those heated for 1 h.
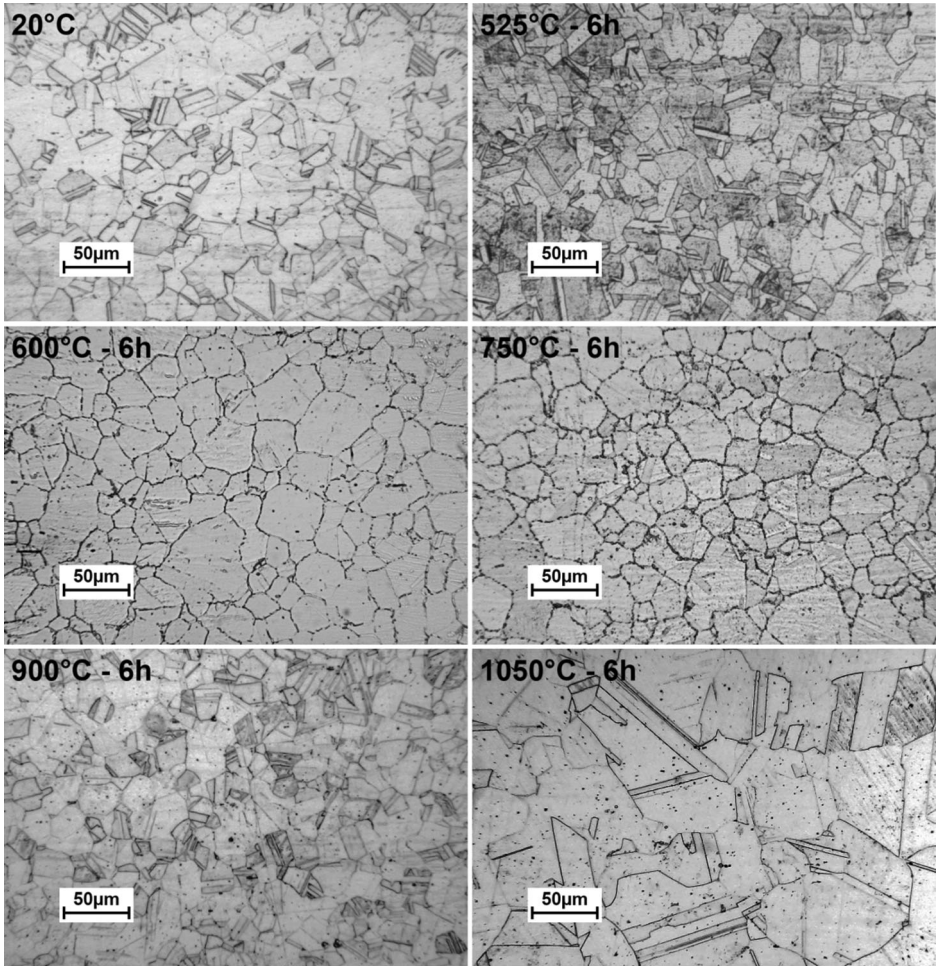
Figure 12. Metallographic survey on the longitudinal direction of the specimens heated for 6 h at 20°C, 525°C, 600°C, 750°C, 900°C, 1050°C (200x). The etching was carried out by a solution containing HCl—45 ml, HNO$_3$—15 ml, glycerol—3 ml and water—30 ml.

The statistical analysis of the color has allowed us to demonstrate that from 20°C to 340°C there are no significant variations in color, as well as between the samples at 900°C and 1050°C. In the range between 340°C and 900°C, each temperature corresponds to a precise color tone both in the case of exposure for 1 h and for 6 h. Between 340°C and 525°C the surface oxides form small spots of a different color compared to the rest of the sheet. This phenomenon can also be exploited to accurately identify the temperature of AISI 316 stainless steel sheets involved in a fire.
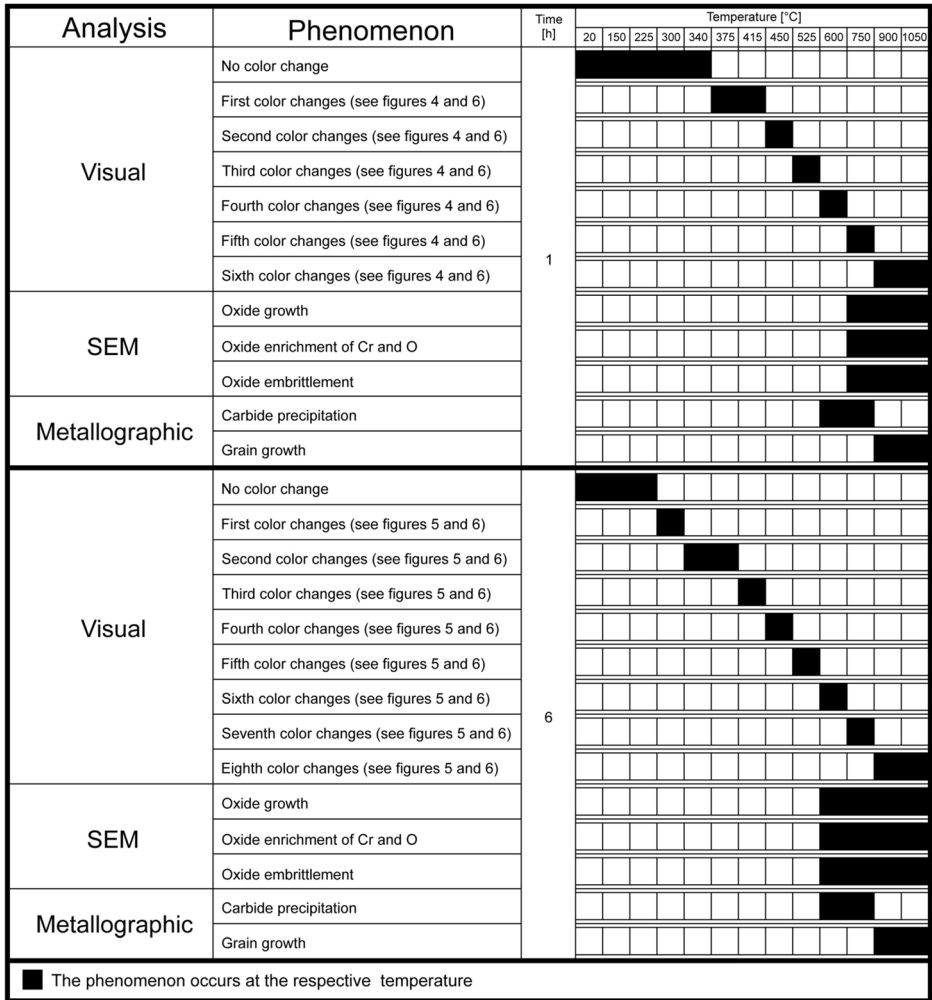
Analysis	Phenomenon	Time [h]	20	150	225	300	340	375	415	450	525	600	750	900	1050
Visual	No color change		█	█	█	█	█								
	First color changes (see figures 4 and 6)							█	█						
	Second color changes (see figures 4 and 6)									█					
	Third color changes (see figures 4 and 6)										█				
	Fourth color changes (see figures 4 and 6)	1										█			
	Fifth color changes (see figures 4 and 6)												█		
	Sixth color changes (see figures 4 and 6)													█	█
SEM	Oxide growth													█	█
	Oxide enrichment of Cr and O													█	█
	Oxide embrittlement													█	█
Metallographic	Carbide precipitation											█	█		
	Grain growth														█
Visual	No color change		█	█	█										
	First color changes (see figures 5 and 6)				█										
	Second color changes (see figures 5 and 6)					█	█								
	Third color changes (see figures 5 and 6)							█							
	Fourth color changes (see figures 5 and 6)								█						
	Fifth color changes (see figures 5 and 6)										█				
	Sixth color changes (see figures 5 and 6)	6										█			
	Seventh color changes (see figures 5 and 6)													█	
	Eighth color changes (see figures 5 and 6)														█
SEM	Oxide growth												█	█	█
	Oxide enrichment of Cr and O												█	█	█
	Oxide embrittlement												█	█	█
Metallographic	Carbide precipitation											█	█		
	Grain growth														█

█ The phenomenon occurs at the respective temperature

Figure 13. Correlation between temperature and modifications observed on the AISI 316 stainless steel sheets.

The SEM/EDS analyzes do not show significant changes in the surface oxide of iron-chromium-nickel and molybdenum naturally formed by stainless steel AISI 316 up to 600°C.

The effects of hot oxidation are evident starting from 750°C. From this temperature the oxide layer begins to grow in an uncontrolled way, greatly increasing its thickness and preferentially enriching with chromium and oxygen. The shape of the oxides also changes dramatically. If up to 600°C the oxide is smooth and compact, starting from 750°C it assumes a rough shape and tends to flake off easily.

The increase in thickness continues both at 900°C and at 1050°C, further enriching with oxygen and chromium and gradually occupying the entire surface of the sample.

Samples subjected to an exposure time of six hours show a similar behavior, even if the growth of the oxide layer already begins at temperature (600°C) lower than the tests performed for 1 h.

The metallographic analysis shows a fully recrystallized equiaxed grain with an average size of 20 μm from 20°C up to 525°C. Between 600°C and 750°C there is a strong precipitation of chromium carbides at the grain boundary, while starting from 900°C there is a marked growth of the average grain size which at 1050°C exceeds 100 μm. On the other hand, there are only limited differences in the microstructure between the tests conducted with a heat exposure time of 1 h or 6 h.

The results discussed in the previous paragraphs allow to create a table that highlights the most important morphological and microstructural alterations by correlating to a given temperature (Fig. 13).

Consequently, the discovery of AISI 316 stainless steel flue pipes at the site of a fire could be of great help in determining the maximum temperatures reached during the fire.

However, some cautionary words are needed to move from laboratory conditions to the real world. It is important to remember that all tested specimens have a reduced thickness, have a homogeneous temperature throughout the thickness and have been air-cooled. For these reasons it is significant to rely on expert judgment in addition to referring to Fig. 13.

Open Access

References

1. (2008) NFPA 921: guide for fire and explosion investigations, National Fire Protection Association (NFPA), Quincy, Massachusetts

2. Ortolani C (2007) Casi di combustioni accidentali—Volumi 1 e 2, Maggioli Editori. Sant'Arcangelo di Romagna, Italia
3. Icove DJ (2017) Kirk's fire investigation, 8th edn. Pearson Education, London
4. Lentini JJ (2006) Scientific protocols for fire investigation. CRC Press - Taylor & Francis Group, Boca Raton
5. De Rosa A, Bottà L, Fiorillo A (2015) La semiotica degli incendi. Nucleo Investigativo Antincendi del Corpo Nazionale Vigili del Fuoco, Roma
6. Almirall JR, Furton KG (2004) Analysis and interpretation of fire scene evidence. CRC Press - Taylor & Francis Group, Boca Raton
7. Stauffer E, Dolan JA, Newman R (2008) Fire debris analysis. Academic Press - Elsevier, San Diego
8. Babrauskas V (2005) Charring rate of wood as a tool for fire investigations. Fire Saf J 40:528–554
9. Icove DJ, DeHaan JD (2006) "Hourglass" burn patterns: a scientific explanation for their formation, International Symposium On Fire Investigation Science and Technology, National Association of Fire Investigators
10. ASM Handbook (2004) Properties and selection: nonferrous alloys and special-purpose materials, vol 2. ASM International, Ohio. ISBN: 978-0-87170-378-1
11 ASM Handbook (2004) Metallography and microstructure, vol 9. ASM International, Ohio. ISBN: 978-0-87170-706-2
12. Callister WD (2000) Material science and engineering: an introduction, 5th edn. Wiley, New York
13. Levinson DW (1977) Copper metallurgy as a diagnostic tool for analysis of the origin of building fires. Fire Technol 13:211–222
14. Chi JH, Peng PC (2017) Using the microstructure and mechanical behavior of steel materials to develop a new fire investigation technology. Fire Mater 41(7):864–870
15. Xie D, Shan G, Lv S (2018) Oxidation behavior of carbon steel in simulated kerosene combustion atmosphere: a valuable tool for fire investigations. Fire Mater 42(2):156–163
16. Boniardi M, Casaroli A (2015) In-depth approach to fire investigations: microstructural analysis of metallic materials. Fire Mater 39:600–618
17. Boniardi M, Casaroli A (2014) Metallurgical modification as a tool for fire invetigations. Appl Fire Sci 23(4):467–493
18. Boniardi M, Casaroli A (2014) Influence of heat on non-ferrous objects: metallurgical analysis in fire scene investigations. Fire Technol 50:1335–1356
19. Casaroli A, Boniardi M, Gerosa R, Rivolta B (2021) Metallurgical analysis as a useful method for fire investigation: the case of galvanized steel sheets. Fire Technol 123:553–570
20. Myers RD (2010) Colorchecker passport technical review, Robin Myers Imaging, chromaxion.com
21. British Stainless Steel Association, Heat tint (temper) colours on stainless steel surface heated in air. https://bssa.org.uk/bssa_articles/heat-tint-temper-colours-on-stainless-steel-surface-heated-in-air/ Accessed 10 Jan 2021
22. EN-10088-2:2014. Stainless steels. Technical delivery conditions for sheet/plate and strip of corrosion resisting steels for general purposes, 2014. http://store.uni.com/catalogo/index.php/en-10088-2-2014. Accessed 10 Jan 2021
23. Maleci M, Fiorillo A (2016) Linee guida e tecniche di repertazione video-fotografica nell'ambito delle attività investigative. Nucleo Investigativo Antincendi del Corpo Nazionale Vigili del Fuoco, Roma

24 Antony J (2003) Design of experiments for engineers and scientists, 1st edn. Butterworth Heinemann, Waltham